The use of linear observers to estimate vehicle states during severe handling manoeuvres

Sven Kleine[1] and **Johannes L. van Niekerk**[2]
(Received October 1996; Final version March 1997)

In this paper a linear observer is developed to estimate the dynamic states of a vehicle during severe handling manoeuvres. The observer is designed with a linear three degree of freedom vehicle model. Pole Placement and LQR strategies are evaluated to select the error feedback gain. It is shown that highly inaccurate results can be obtained when the observer gain is chosen blindly. The ability of the observer to estimate vehicle states at high lateral accelerations is demonstrated by means of simulation, using a non-linear three degree of freedom vehicle model. Furthermore, experimental data are used as input to the observer to verify that it is able to estimate the states of an actual vehicle during a single lane change manoeuvre. The observer is found to accurately estimate the vehicle states even at high lateral acceleration.

Nomenclature

Alphabetical symbols

a	distance from c.g. to front axle
$\mathbf{A}$	state dynamic matrix
a_y	lateral acceleration
b	distance from c.g. to rear axle
$\mathbf{B}$	state input matrix
C_0	zero'th tyre moment coefficient
C_1	first tyre moment coefficient
C_2	second tyre moment coefficient
C_{af}	front tyre cornering stiffness
C_{ar}	rear tyre cornering stiffness
C_ϕ	roll damping coefficient
$\mathbf{C}$	state output matrix
$\mathbf{D}$	input-output coupling matrix
$\mathbf{E}$	lateral damping matrix
F_y	lateral force
F	force (depending on subscript)
I_{xx}	moment of inertia about x axis
I_{zz}	moment of inertia about z axis
I_{xz}	roll cross yaw inertia
K_ϕ	roll stiffness coefficient
$\mathbf{K}$	lateral stiffness matrix
M	vehicle total mass
M_s	vehicle sprung mass
M_{uf}	front unsprung mass
M_{ur}	rear unsprung mass
M_x	moment about x axis
M_z	moment about z axis
$\mathbf{M}$	vehicle system mass matrix
p	roll rate
q	pitch rate
r	yaw rate
u	vehicle velocity, varying in time
$\mathbf{u}$	input vector
U	vehicle velocity, constant
v	sideslip velocity, time varying
$\mathbf{x}$	state vector
$\mathbf{y}$	state output vector
z_t	height of the c.g. above the roll axis

Greek symbols

α	general slip angle
α_f	front slip angle
α_r	rear slip angle
β	vehicle sideslip angle
δ_f	front steering input
δ_r	rear steering input
ϕ	roll angle
ψ	yaw angle
θ	pitch angle
τ	front and rear steer time constant

Subscripts

a	referring to acceleration
lf	pertaining to left front tyre
rf	pertaining to right front tyre
lr	pertaining to left rear tyre
rr	pertaining to right rear tyre
o	referring to observer

Terminology

DOF	degree of freedom
c.g.	centre of gravity
LQR	linear quadratic regulator
SBW	steer by wire
2DOF	two degree of freedom
3DOF	three degree of freedom
4WS	four wheel steer

Introduction

In the past few decades vehicle systems have increased significantly in complexity. Active control is used to manipulate various vehicle states such as engine torque, braking

[1] Post-graduate student

[2] Associate Professor, SASOL Chair in Vehicle Engineering, Department of Mechanical and Aeronautical Engineering, University of Pretoria, Pretoria, 0002 South Africa. (Member)

forces and, more recently, the steering angles on all four wheels.[1,2,3] This increase in controller complexity implies that many more vehicle states are required to effectively determine the optimal control signals. A number of these control systems even make use of full state feedback which implies that all the vehicle states must be accessible.[4,5,6] However, very little research has been done on how to obtain these various states.[7] In fact, some of these states are not directly measurable and hence must be estimated from those states that can be measured. It is for this reason that research has been focused on designing a linear observer to estimate all the vehicle states. This work, and work performed in Senger *et al.*[8] and Kleine,[9] provides new insight into the use of observers as applied to vehicles.

One of the vehicle states that is often used in active vehicle control systems is the slip angle of the vehicle's tyres. This quantity is extremely difficult to measure directly and one has no alternative but to obtain it from other vehicle states. As tyre side force is a function of slip angle it is also an important parameter for the motorsport fraternity whose primary concern is to maximise the forces between the tyres and the road. If all the vehicle states are available it will be possible to estimate the slip angle at each wheel from the available information.

The observer that is discussed in this study is a linear Luenberger observer. However, it is used to observe the dynamics of both a linear and a non-linear vehicle model. After verifying the ability of the system to observe all the vehicle states in simulation the observer is used to analyse experimental data.

Vehicle model

For this study it was necessary to develop both a linear and a non-linear vehicle model.

Linear Vehicle Model

The linear vehicle model used in this paper is similar to that developed in Kleine.[9] This model is an extension of one first proposed by Von Riekert and Schunk,[10] which has been updated by Allen *et al.*,[11] and became the standard used by many other researchers.[12,13] The states of the system are yaw rate (p), sideslip velocity (v), and roll rate (r) which corresponds to the three degrees of freedom of the model (see Figures 1 and 2).

To develop the equations of motion a road axis system (X, Y, Z), fixed in space, is chosen. A vehicle fixed axis system (x, y, z) is attached to the sprung mass on the roll axis, below the centre of gravity. The x axis points forward, y axis to the left and z axis upwards.

For linear analysis, self-aligning moments of tyres, load transfer effects, roll steer, and roll induced camber are neglected. The linear equations are obtained using the Newton-Euler approach:

$$M\dot{v} + MUr + M_s z_t \dot{p} = \sum F_y \qquad (1)$$

$$I_{xx}\dot{p} + M_s z_t \dot{v} + M_s z_t U r + I_{xz}\dot{r} = \sum M_x \qquad (2)$$

$$I_{zz}\dot{r} + I_{xz}\dot{p} = \sum M_z \qquad (3)$$

The use of a linear model also implies that a linear tyre model must be used. The forces acting on the vehicle are given by:

$$\sum F_y = -2C_{\alpha f}\alpha_f - 2C_{\alpha r}\alpha_r \qquad (4)$$

$$\sum M_x = -C_\phi p - K_\phi \phi + M_s g z_t \phi \qquad (5)$$

$$\sum M_z = -2aC_{\alpha f}\alpha_f + 2bC_{\alpha f}\alpha_r \qquad (6)$$

These equations can be written in the state space as:

$$\begin{aligned} \dot{\mathbf{x}} &= \mathbf{Ax} + \mathbf{Bu} \\ \mathbf{y} &= \mathbf{Cx} + \mathbf{Du} \end{aligned} \qquad (7)$$

where $\mathbf{x} = [y\ \phi\ \psi\ v\ p\ r]^T$ and $\mathbf{u} = [\delta_f\ \delta_r]^T$. The state matrices are derived in the appendix. The $\mathbf{C}$ and $\mathbf{D}$ matrices are specified according to which states are required as output. The states used throughout represent:

- y lateral position
- $\dot{y} = v$ sideslip velocity
- ϕ roll angle
- $\dot{\phi} = p$ roll rate
- ψ yaw angle
- $\dot{\psi} = r$ yaw rate

The advantage of representing the model in the familiar state space format is that it is much more amenable to modern control design techniques. The full derivation of these linear equations is presented in Kleine.[9]

Non-linear vehicle model

To obtain more accurate simulation results it is necessary to use a more realistic vehicle model. Such a model will include the non-linear behaviour of tyre forces as well as the varying load distribution due to vehicle roll. For this purpose a non-linear, four-wheel, three degree of freedom model was developed.

The following assumptions were made to simplify the equations of motion:

- Assume the vehicle is moving on a plane surface, the vertical motion of the sprung mass (M_s) and the two unsprung masses (M_{uf} and M_{ur}) can be ignored.
- For simplicity, the roll motions of the unsprung masses, and the pitch motion of the sprung mass are not included in the model.

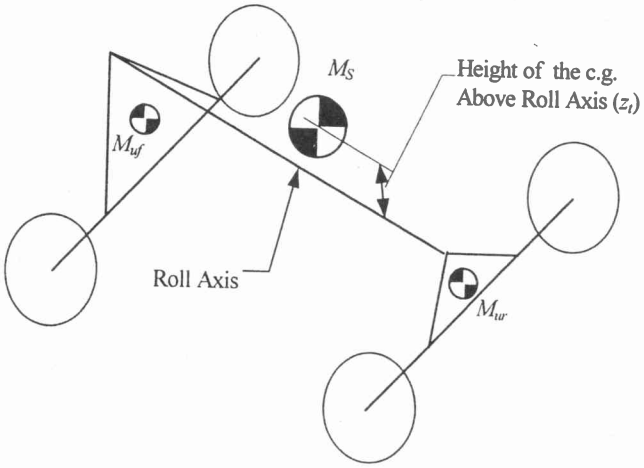

Figure 1 Three degree of freedom model

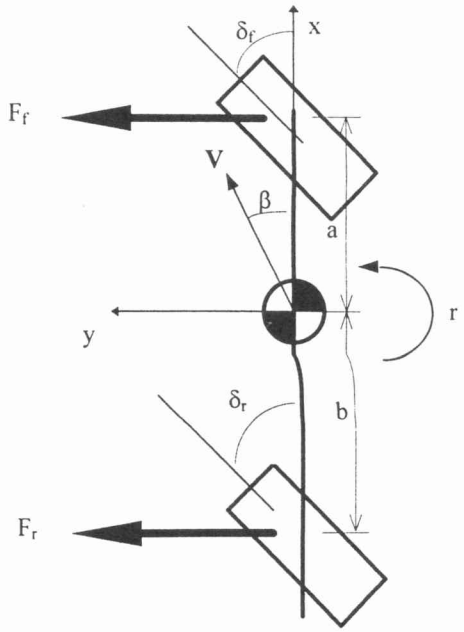

Figure 2 Top view of Three Degree of Freedom, with left and right wheels combined at centre of vehicle

- The vehicle is modelled by three masses (defined above) which are connected by a roll axis at a fixed height. (Although in reality this height will vary slightly as the suspension deflects during body roll.)[13]

The dominant force generating mechanism is the friction between the road and the tyres. To correctly model the vehicle dynamics requires an accurate tyre model. The non-linear tyre model used in this study is an extension of the friction ellipse concept presented in Whitehead[12] and Dugoff *et al.*[14] and the detail can be found in Kleine.[9] The tyre force is calculated based on vertical load, lateral slip angle, longitudinal slip ratio and vehicle speed. Other significant input parameters are inflation pressure, static and dynamic coefficient of friction.

The equations of motion are developed according to the previous assumption using the Newton-Euler approach. The non-linear equations of motion are the same as those represented by equations (1), (2), and (3). However, these equations are now coupled through the non-linear tyre forces

$$\sum F_y = (F_{ylf} + F_{yrf})\cos\delta_f + (F_{ylr} + F_{yrr})\cos\delta_r \quad (8)$$

$$\sum M_x = -C_\phi p - K_\phi \phi + M_s g z_t \phi \quad (9)$$

$$\sum f_y = -a(F_{ylf} + F_{yrf})\cos\delta_f + b(F_{ylr} + F_{yrr})\cos\delta_r \quad (10)$$

The slip angles, α, that are used in the non-linear, non-dimensional tyre function, are non-linear functions of the vehicle states represented by the following equations:

$$\alpha_f = \arctan\left(\frac{v + ar}{u}\right) - \delta_f \quad (11)$$

$$\alpha_r = \arctan\left(\frac{v - br}{u}\right) - \delta_r \quad (12)$$

The effect of lateral load transfer is modelled according to the approach in Kleine,[9] the load transfer at each wheel is calculated as a function of roll angle, lateral acceleration and the front to rear distribution of mass. It is well known that tyres do not generate side-force instantaneously and therefore this is modelled by an additional first order lag. The dynamic time lag of the tyre forces is modelled according to Heydinger *et al.*,[15] with the detail presented in Kleine.[9]

For accuracy and repeatability a driver model is required. The driver model used in this study is a dual level model, using a second order path prediction function (with anticipatory open loop and compensatory closed loop dynamics), and variable driver gain. The complete model is discussed in Kleine.[9]

Observer

Design

The linear model developed in the previous section will be used to design the observer. It has the major advantage of simplicity and ease of use.

The use of observers in control system design and simulation is not a new concept. It was introduced by Luenberger in the sixties. However, the use of observers in the field of vehicle dynamics has not received a lot of attention. The use of full-state feedback is often used to effect vehicle dynamics through traction control and 4WS. There appears to be an inconsistency in the literature since full state feedback systems would require some form of observer to estimate all of the states but from the literature available it becomes clear that very little work has been done to develop such observers.

The most likely sensor to be used in a vehicle is an accelerometer. It will be possible to measure the roll and yaw rate using rate gyros and the sideslip velocity can be measured using a suitable velocity transducer. These types of sensors are however expensive and will therefore not be used on mass produced vehicles. Furthermore, some of the states such as y and ψ are just about impossible to measure. When approached from the point of view of cost, ease of implementation and safety, the most likely measurement sensor would be an accelerometer. This accelerometer would measure the lateral acceleration of the vehicle. There is however a disadvantage as lateral acceleration is not a state of the system; it can only be obtained as a combination of states and their derivatives.

From the equations of motion, (1) and (2), it can be seen that lateral acceleration is represented by the following equation:

$$a_y = \dot{v} + Ur + z_t\dot{p} \quad (13)$$

- where $\dot{v} = \ddot{y}$ the derivative of state 4,
- and $r = \dot{\psi}$ state 6,
- and $\dot{p} = \ddot{\phi}$ the derivative of state 5.

Hence, should one incorporate these into the system matrices, it will result in a non-zero **D** matrix. This is undesirable as many control theories are based on a plant with no direct feedforward term.

To overcome this problem the following simple, yet elegant, mathematical manipulation can be carried out. It consists of introducing additional states $\tilde{\mathbf{u}}$ which are the result of low pass filtering the input **u**. Hence if $\tilde{\mathbf{u}}$ are used instead of **u** when computing the derivatives the need for a non-zero **D** matrix can be pre-empted. Applying this low pass filtering to the two inputs, front (δ_f) and rear (δ_r) steering:

$$\dot{\tilde{\delta}}_f = \frac{-1}{\tau_1}\tilde{\delta}_f + \frac{1}{\tau_1}\delta_f \quad (14)$$

$$\dot{\tilde{\delta}}_r = \frac{-1}{\tau_2}\tilde{\delta}_r + \frac{1}{\tau_2}\delta_r \quad (15)$$

and then representing this as a first order system in the state space format:

$$\dot{\tilde{\mathbf{u}}} = \begin{bmatrix} -\frac{1}{\tau_1} & 0 \\ 0 & -\frac{1}{\tau_2} \end{bmatrix} \tilde{\mathbf{u}} + \begin{bmatrix} -\frac{1}{\tau_1} & 0 \\ 0 & -\frac{1}{\tau_2} \end{bmatrix} \mathbf{u} \qquad (16)$$

it is possible to augment these equations to eliminate the **D** matrix. The new states are:

$$\tilde{\mathbf{x}} = \begin{bmatrix} \mathbf{x} \\ \tilde{\mathbf{u}} \end{bmatrix} \text{ where } \tilde{\mathbf{u}} = \begin{bmatrix} \tilde{\alpha}_f \\ \tilde{\alpha}_r \end{bmatrix} \qquad (17)$$

It is important to define τ_1 $(i = 1, 2)$ so that $\tilde{\mathbf{u}} \approx \mathbf{u}$, this requires that the filter frequency be much higher than the fastest mode of the system. The selection of these time constants is discussed in more detail in the next section which is concerned with the selection of the design parameters. The modal frequencies are computed from the **A** matrix of the vehicle state space model defined in the appendix.

The lateral acceleration can now be expressed as follows:

$$a_y = [\mathbf{C}_a]\,\mathbf{x} + [\mathbf{D}_a]\,\tilde{\mathbf{u}} \qquad (18)$$

with $\mathbf{C}_a$ and $\mathbf{D}_a$ as defined in the appendix.

If $\tilde{\mathbf{u}}$ is now appended to the vehicle states the output equation will contain only vehicle states and the matrix **C** can be defined as follows

$$a_y = [\mathbf{C}_0]\,\tilde{\mathbf{x}} \text{ with } \mathbf{C}_0 = [\mathbf{C}_a \quad \mathbf{D}_a] \text{ and } \tilde{\mathbf{x}} = \begin{bmatrix} \mathbf{x} \\ \tilde{\mathbf{u}} \end{bmatrix} \qquad (19)$$

and now finally $\mathbf{D} = [0]$. So that the equations in full are given by:

$$\dot{\tilde{\mathbf{x}}} = \begin{bmatrix} \begin{bmatrix} A_{11} & & & & & A_{16} \\ \vdots & \cdots & \cdots & \cdots & \cdots & \vdots \\ \vdots & \ddots & & & & \vdots \\ \vdots & & \ddots & & & \vdots \\ \vdots & & & \ddots & & \vdots \\ \vdots & & & & \ddots & \vdots \\ \vdots & \cdots & \cdots & \cdots & \cdots & \vdots \\ A_{61} & & & & & A_{66} \end{bmatrix} & \begin{matrix} 0 & 0 \\ 0 & 0 \\ 0 & 0 \\ 0 & 0 \\ 0 & 0 \\ 0 & 0 \end{matrix} \\ \begin{matrix} 0 & 0 & 0 & 0 & 0 & 0 \\ 0 & 0 & 0 & 0 & 0 & 0 \end{matrix} & \begin{matrix} \frac{-1}{\tau_1} & 0 \\ 0 & \frac{-1}{\tau_2} \end{matrix} \end{bmatrix} \tilde{\mathbf{x}} + \begin{bmatrix} \begin{bmatrix} B_{11} & B_{12} \\ \vdots & \vdots \\ \vdots & \vdots \\ \vdots & \vdots \\ \vdots & \vdots \\ \vdots & \vdots \\ B_{61} & B_{62} \end{bmatrix} \\ \begin{matrix} \frac{1}{\tau_1} & 0 \\ 0 & \frac{1}{\tau_2} \end{matrix} \end{bmatrix} \mathbf{u} \qquad (20)$$

$$\mathbf{y} = [\mathbf{C}_0]\,\tilde{\mathbf{x}} + [\mathbf{0}]\,\mathbf{u} \qquad (21)$$

Block diagram

In the state space this becomes

$$\dot{\tilde{\mathbf{x}}} = \mathbf{A}_0\tilde{\mathbf{x}} + \mathbf{B}_0\mathbf{u} \qquad (22)$$

$$\mathbf{y} = \mathbf{C}_0\tilde{\mathbf{x}} + \mathbf{D}_0\mathbf{u} \qquad (23)$$

Now the matrices can be represented in the generic observer block diagram, see Figure 3.

The gains for matrix L have to be determined to ensure that the system is stable and is fast enough to track the actual vehicle states.

Gain Selection

During the design of the observer, mention is made of the fact that the time constant τ_i needs to be chosen to be faster than the fastest pole in the **A** matrix, or:

$$\tau_i \ll T_n \text{ where } T_n = \frac{2\pi}{\omega_n} \text{ where } n = 1 \text{ to } 6 \qquad (24)$$

In this case (the case of the vehicle), it implies that the dynamics of the filtered states must be 'faster' than that of the system. In a mathematical sense this means that the time constants must be faster than the fastest eigenvalue of the state matrix. For the linear vehicle used in this case, the eigenvalues are given in Table 1 and the time constants that were used are:

$$\tau_1 = 0.01 \text{ and } \tau_2 = 0.0125.$$

These constants cannot be made arbitrarily large because this leads to numerical ill-conditioning of the matrix leading to inaccurate simulations.

It was observed that the system was unobservable. This precluded a pole placement strategy.[15] Examining the system matrices it can be seen that the states y and ψ are unobservable. Physically this makes sense due to the fact that the position of the vehicle and its attitude before a manoeuvre do not affect the dynamics in any way, nor is it present in the information obtained from an accelerometer. These two states can be removed, resulting in a sixth order system.

Observability in this case is also strongly influenced by the presence of only one sensor. It is obvious that, should the vehicle yaw about an axis through the accelerometer, the yaw component will not be sensed. A similar argument can be made for roll. From this it can be postulated that two accelerometers might be needed, placed far from each other, or if only one is used it must be far removed from

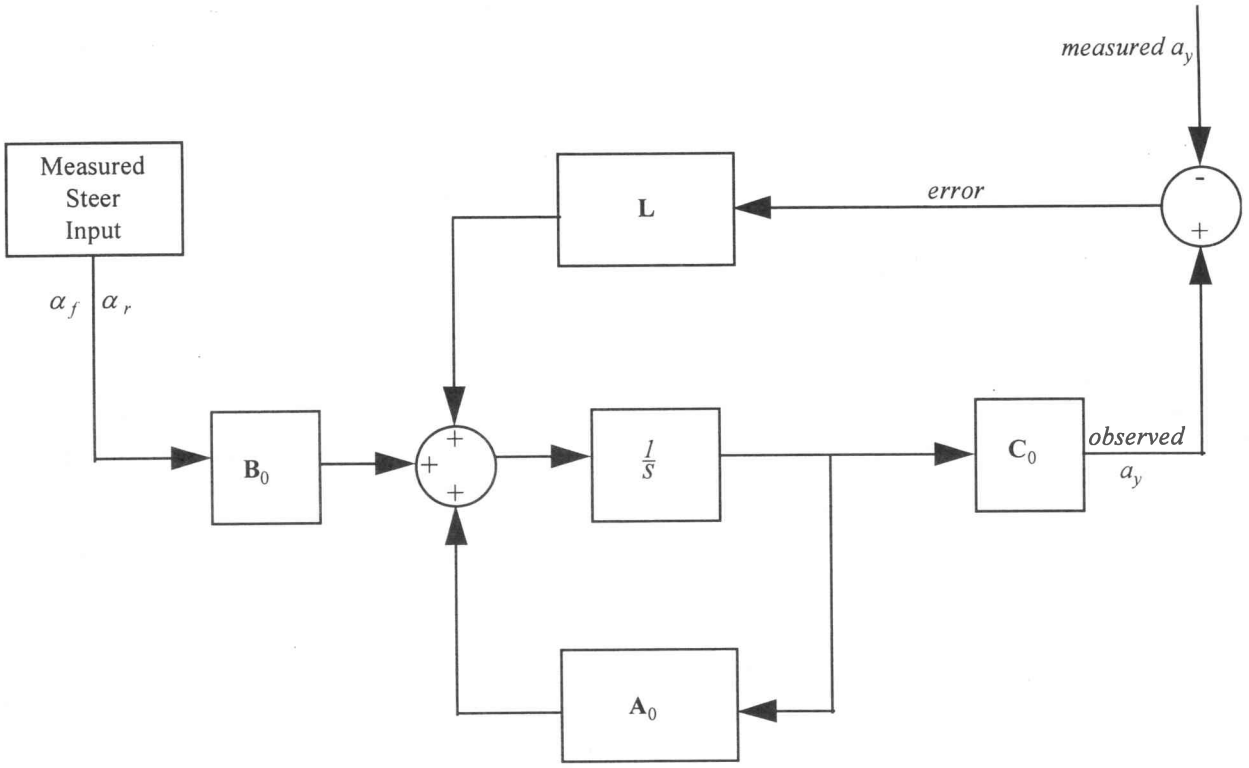

Figure 3 Schematic of control structure of observer

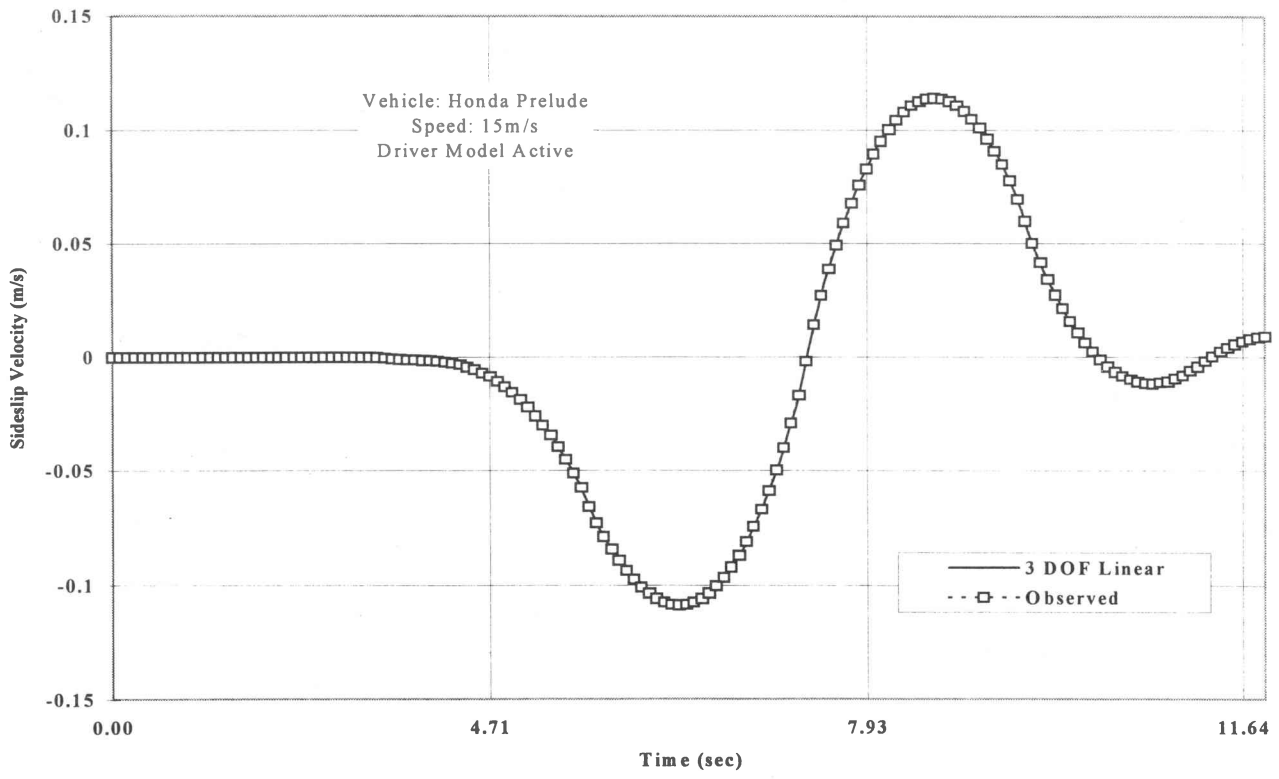

Figure 4 Performance of the observer in tracking sideslip velocity of the linear vehicle model

the possible roll and yaw axis. However, in this particular case, the placement of the accelerometer on the c.g. was found to be satisfactory.

Once the time constants have been set and the matrix reduced to make it observable the open-loop eigenvalues decrease in number, Table 1.

Table 1 Vehicle Eigenvalues before and after reduction of states

	non-reduced	reduced
ω_1	0	-20.78
ω_2	0	-1.726
ω_3	-20.78	-100
$\omega_4$and ω_5	$-7.254 \pm i6.593$	$-7.524 \pm i6.593$
ω_6	-1.726	-80
ω_7	-100	
ω_8	-80	

The closed loop poles can now be placed using established procedures. The equation for which to place the poles is (15)

$$\dot{\mathbf{e}} = (A - \mathbf{LC})\,\mathbf{e} \tag{25}$$

where $e = \mathbf{x} - \tilde{\mathbf{x}}$ is the error between the observed and the actual vehicle states.

The feedback matrix **L** can be determined by placing the poles of the closed loop system in the desired locations. Equation (36) represents the error dynamics of the system, with **e** being the error between the actual and estimated vehicle states. Should the poles for this system be placed to have negative eigenvalues, it will represent a stable system, with the error decaying to zero, as desired. The location of the poles is chosen to ensure that the closed loop error dynamics are significantly faster than that of the open loop system.

As a first attempt the pole placement was performed using the pole placement algorithm, 'place' in Matlab, and also the more robust algorithm 'acker' using Ackerman's formula. The resulting closed loop eigenvalues and gains are given in Table 2 and Table 3. These algorithms led to large gains, simulation instability and numerical problems.

Table 2 Eigenvalues of the closed loop error dynamics

c	Using PLACE	Using LQR
ω_1	-400	-917
ω_2	-378	$-73.9 + j11.3$
ω_3	-328	$-73.9 + j11.3$
ω_4	$-306 + j13,3$	$-21.5 + j5.60$
ω_5	$-306 + j13,3$	$-21.5 + j5.60$
ω_6	-295	-85

The next approach was to make use of linear quadratic regulator (LQR) theory to obtain the gain matrix. The theory behind this type of gain determination is well established and can be found in papers such as Heydinger *et al.*[15] It falls into the category of modern control theory and makes use of state space techniques.

Table 3 Elements of the L matrix which is an indication of the gain of the observer

Gain	Using PLACE	Using LQR
L_{11}	950	0.7527
L_{12}	-2752000	-37.54
L_{13}	25760000	17.52
L_{14}	8445200	20.19
L_{15}	$-2209,9$	8.424
L_{16}	7227,4	2.520

The pivotal point of this strategy is the minimisation of a specified performance criterion J. This is the integral of a quadratic form in the state **e**, plus a second quadratic form in the control **y** (measurement error in this case) i.e.

$$J = \int_0^\infty [\mathbf{e}'(\tau)\,\mathbf{Q}(\tau)\,\mathbf{e}(\tau) + \mathbf{y}'(\tau)\,\mathbf{R}\mathbf{y}(\tau)]\,d\tau \tag{26}$$

Q must be positive semi-definite and **R** positive definite. These are often called the state weighting matrix and control weighting matrix, respectively. In the performance criterion these two matrices determine the cost of control, i.e. **Q** represents the cost, or penalty of deviating from the required state. **R** represents the cost of controlling this deviation. Hence, their ratio determines the gain of the resulting controller.

At first the **Q** matrix was selected as follows:

$$\mathbf{Q} = diagonal\,[40 \quad 40 \quad 40 \quad 40 \quad 10 \quad 10] \tag{27}$$

This too only had limited success, and resulted in similar problems to those experienced with the 'place' and 'acker' algorithms.

This failure led to a re-evaluation of the gain selection procedure. It came to light that the initial method was to select gains by placing the poles for the error dynamics in the desired places. This, however, led to an inconsistency in the control. This inconsistency comes about as a result of attempting to control the error in $\tilde{\phi}$ and $\tilde{p}$ *independently* through the gain matrix. These terms are *dependent* on each other, as $\tilde{\phi}$ is just the integral of $\tilde{p}$. Thus it follows that only $\tilde{\phi}$ or $\tilde{p}$ needs to be controlled, the other dependent term will automatically follow through the dynamics of the **A** matrix. Based on this the new **Q** was chosen as

$$\mathbf{Q} = diagonal\,[0 \quad 40 \quad 40 \quad 40 \quad 1 \quad 1] \tag{28}$$

These resulting gains and closed loop eigenvalues are summarised in Tables 2 and 3.

It can be clearly seen that the LQR strategy resulted in substantially smaller gains than when trying to place the poles of the observer directly.

Results

To judge the ability of the observer to follow the actual vehicle states the following scenarios were investigated:

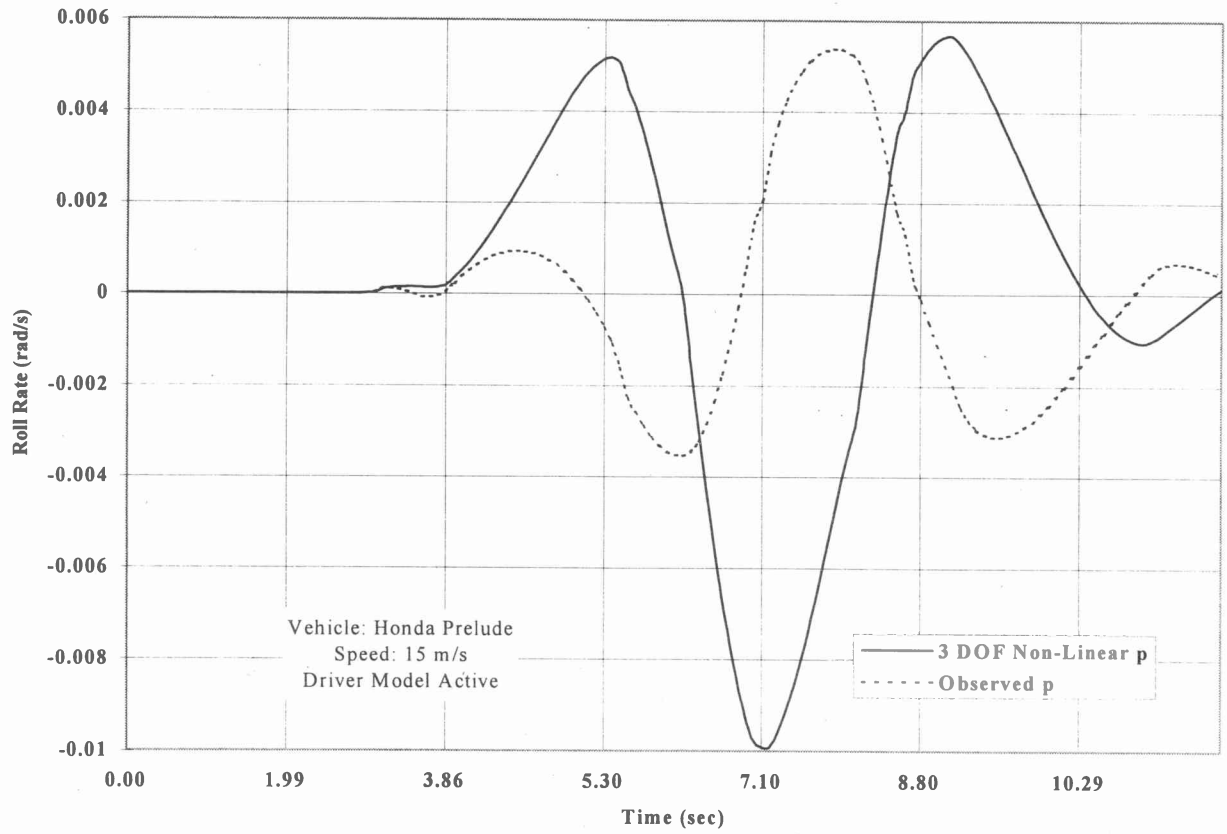

Figure 5 Failure of the observer in tracking the roll rate of the non-linear model (before LQR gain selection)

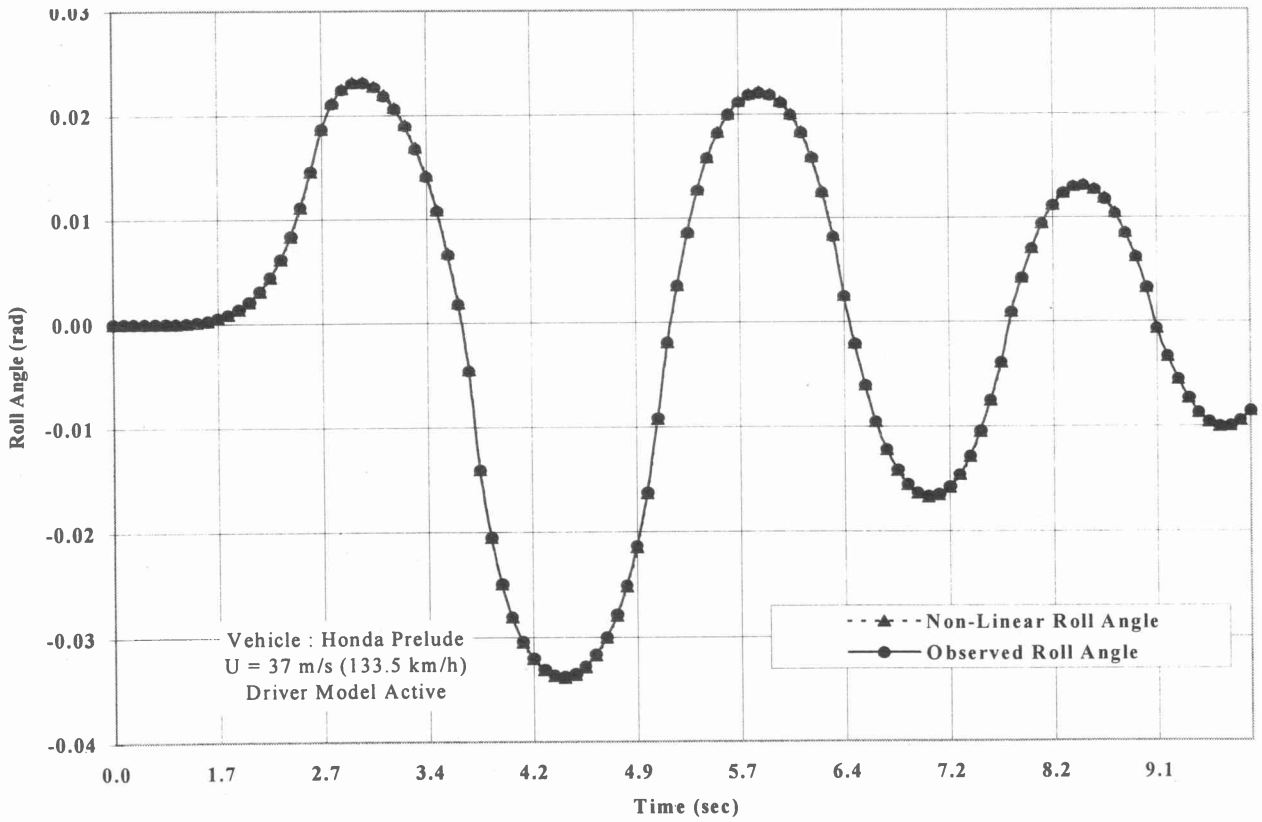

Figure 6 Performance of the observer in tracking roll angle of the non-linear vehicle model

1. The linear observer tracking the linear vehicle model
2. The linear observer tracking the non-linear vehicle model
3. The linear observer estimating the vehicle states from experimental data

Linear vehicle model

The first case consists of observing the states of the linear vehicle model while performing a single lane change in accordance with ISO/TR3888. As expected the vehicle and the observer states match each other perfectly since the same model was used in the design of the observer. Figure 4 shows the estimation of the sideslip and is indicative of the observer's ability to observe the states with zero error.

Non-linear vehicle model

The object of this study was to design an observer to observe the vehicle states of a non-linear vehicle. To simulate this scenario the non-linear vehicle model developed as described earlier was used. The results of these simulations are presented in Figures 5 to 9. It should be noted that the speed of the vehicle has been increased to 37 m/s, this is 133,5 km/h. At this speed non-linear vehicle and tyre characteristics begin to manifest themselves. This is necessary to determine whether the observer is able to estimate the vehicle states adequately during severe handling manoeuvres.

In the graphs displayed in Figures 5 to 9 a comparison is made of the observer performance before the successful gain strategy and thereafter. Figure 5 shows the roll rate estimation of the unsuccessful gain determination strategy (pole placement), while Figure 8 shows the successful roll rate estimation using the LQR approach. With the unsuccessful approach the roll angle appeared to be accurately observed, however the roll rate was unacceptable. With the LQR approach the estimation of roll rate improved significantly as can be seen in Figure 8, the estimation of roll angle using the LQR approach also improves, Figure 6. The simulation parameters used for the vehicle before the LQR approach and after remain unchanged and all improvements are solely due to the observer. With the LQR strategy the performance of the observer is exceptional even under a manoeuvre as severe as this one; this can be seen by the yaw rate (Figure 9) which has very little deviation.

The fact that this single lane change is indeed severe is indicated by the graph of lateral acceleration (Figure 10) which shows lateral accelerations in excess of 4 m/s^2. According to Allen & Rosenthal[17] manoeuvres in excess of 4 m/s^2 are sufficient to induce truly non-linear characteristics and cause non-linear behaviour to be displayed. The ability of the observer to perform its function very well is undisputed in light of the results of the vehicle performing a very severe lane change manoeuvre. The severity of this manoeuvre can also be shown by the fact the vehicle displays oscillatory behaviour at the end of the lane change as shown by the various vehicle states after 6 seconds. Even during this high frequency yaw motion the observer still performs its task satisfactorily.

Estimation of sideslip velocity (Figure 7) is slightly compromised during high lateral acceleration. This can be attributed to the fact that when the tyres begin to saturate the non-linear vehicle is unable to generate force at the rate it would under lower acceleration. This implies that the velocity must begin to decrease. In the observer, which has a linear tyre model, this reduction does not occur, and thus the ability to converge on the correct value is compromised although it can be seen that the error is less than 15%, at a lateral acceleration of 0.52 g.

Experimental results

To verify the observer using real vehicle data a single lane change test was conducted with a Volkswagen Golf. During the experiment the following measurements were taken: steering angle, lateral acceleration, yaw rate, and roll rate. Using only the acceleration (Figure 13) and steering angle (Figure 14) data as input to the observer all the states were estimated. The results are presented in Figures 11 and 12.

Here the manoeuvre that was performed is not as severe as that performed in the previous simulations due to safety concerns. However, the data presented here still represent a severe lane change at 90 km/h. The results indicate that the estimated and measured yaw and roll rates correlate well. The observer has the ability to estimate the yaw and roll rate of the vehicle very accurately. The higher order dynamics as well as the lower order dynamics are present in the estimated signals. The only deficiency that can be seen is that the magnitude of the estimated signal is not always the same as the measured state. This can be attributed to the fact that accurate data for the vehicle tyres were not available and the values used for $C_{\alpha f}$ and $C_{\alpha r}$ are probably higher than they should be. This will lead to higher observed values for short periods of time at high lateral accelerations as can be seen here.

Conclusion

A linear Luenberger observer was designed in this study which makes use of a single acceleration measurement to estimate all the important vehicle states for lateral vehicle dynamics. Even at high lateral accelerations the observer demonstrated that in simulation it can be used to estimate the states of a non-linear vehicle model. Finally, experimental data were used to verify the ability of the observer to estimate the vehicle states making use of actual measured acceleration data.

In this study it came to light that the implementation of the observer has to be carefully executed. The values of parameters such as the time constants of the system

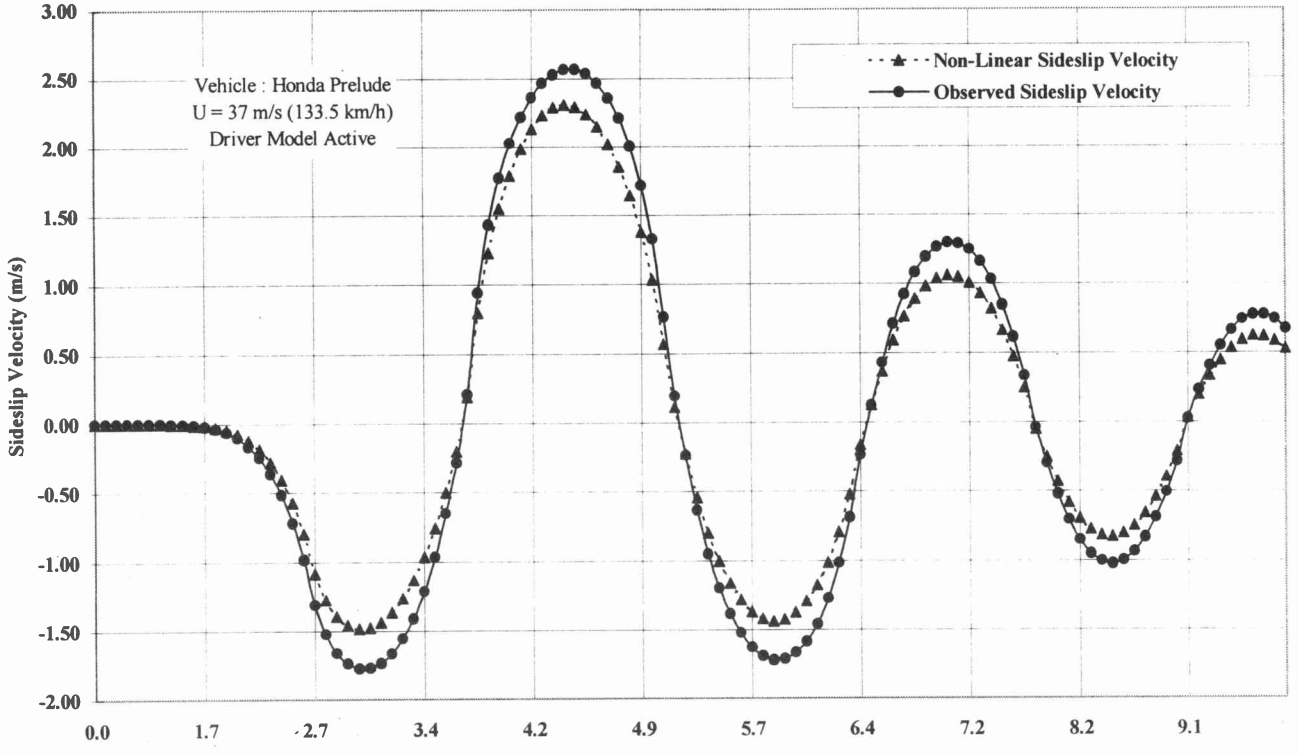

Figure 7 Performance of the observer in tracking sideslip velocity of the non-linear vehicle model

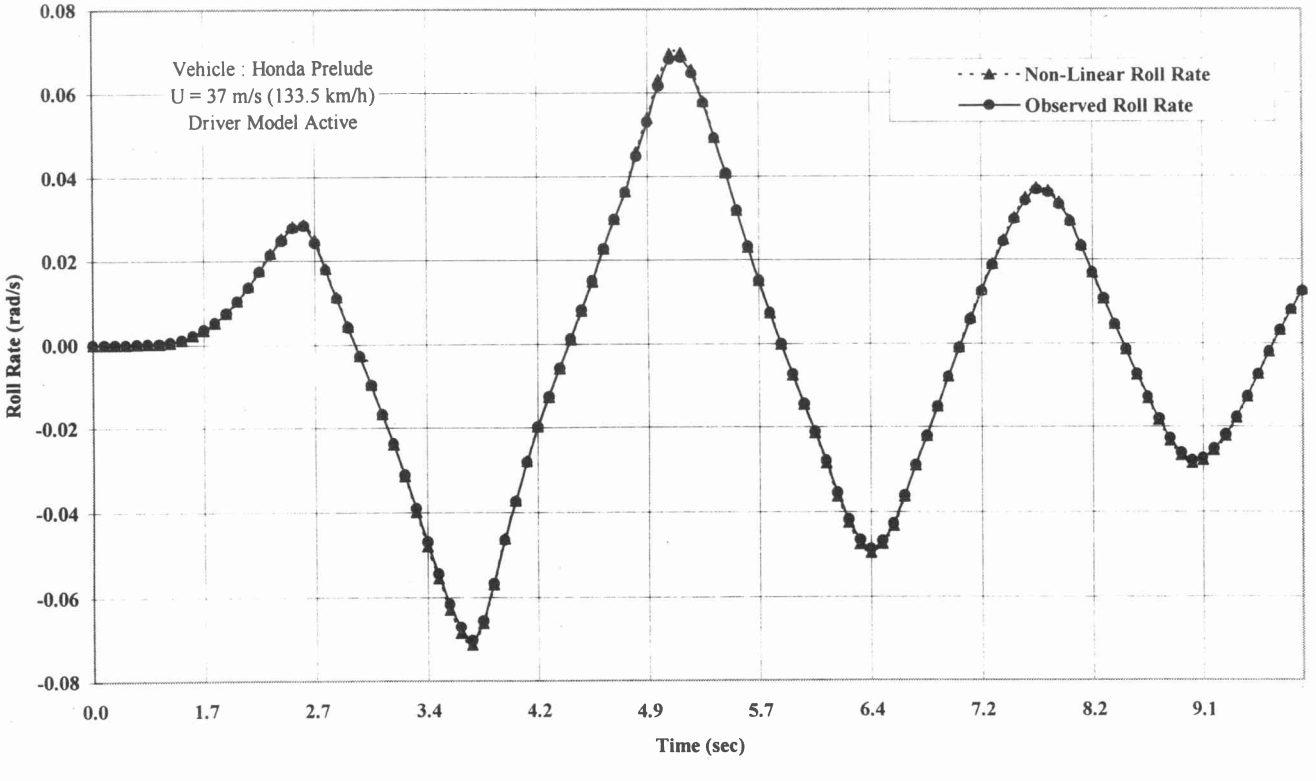

Figure 8 Performance of the observer in tracking roll rate of the non-linear vehicle model (after LQR gain selection)

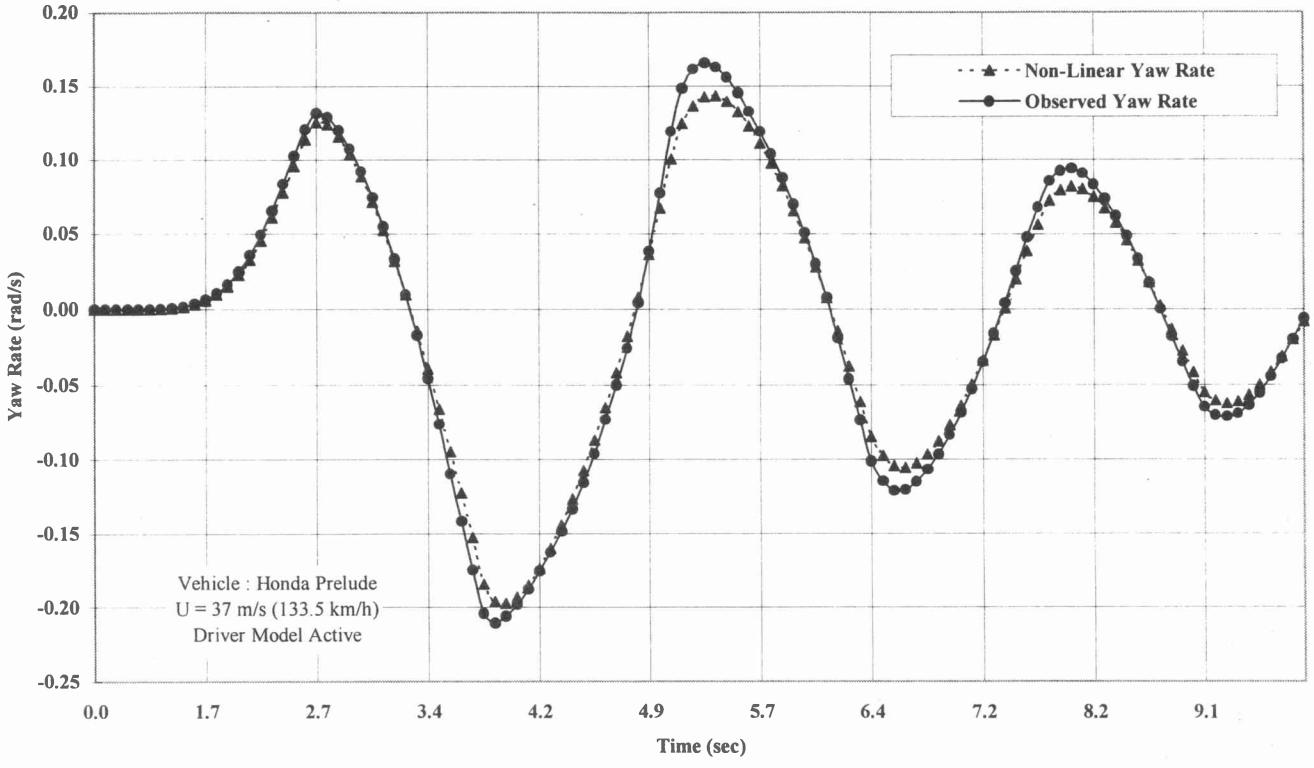

Figure 9 Performance of the observer in tracking the yaw rate of the non-linear vehicle model at high lateral acceleration

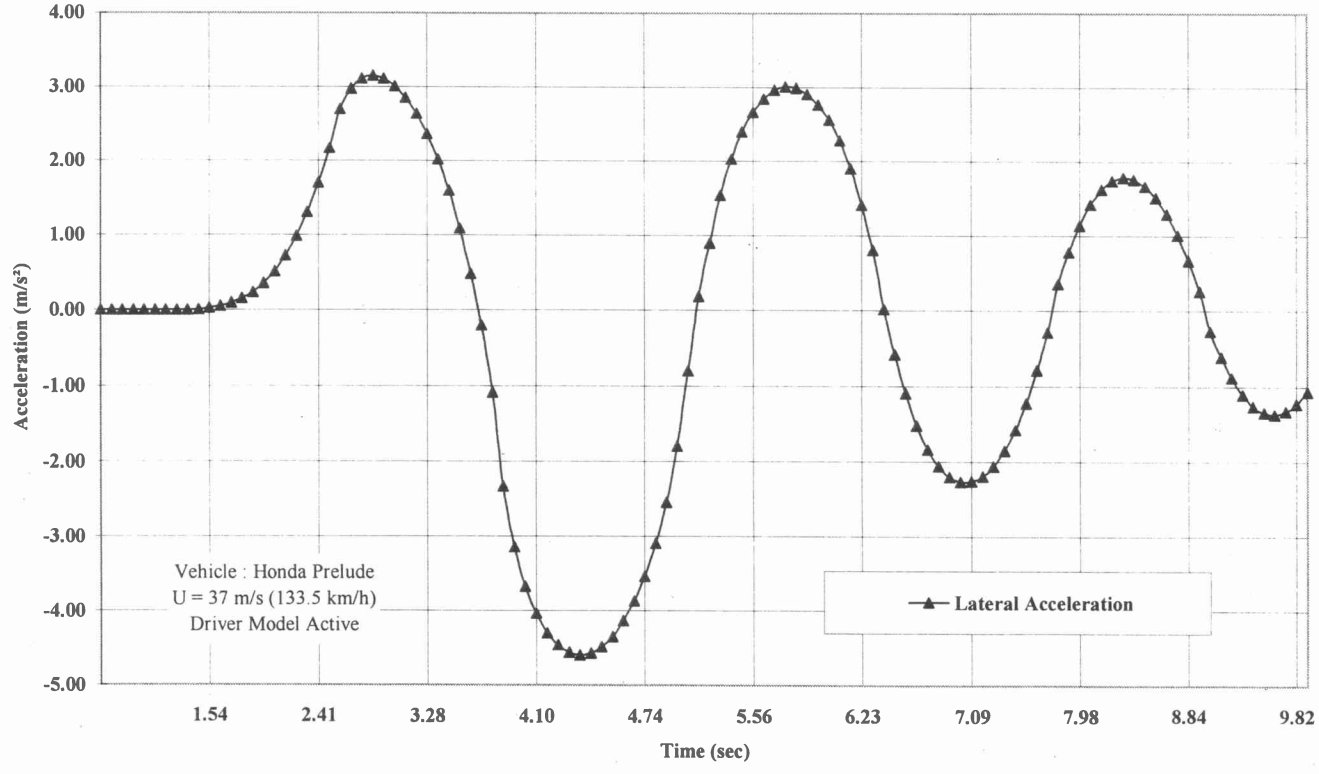

Figure 10 Performance of the observer remains not compromised at high accelerations

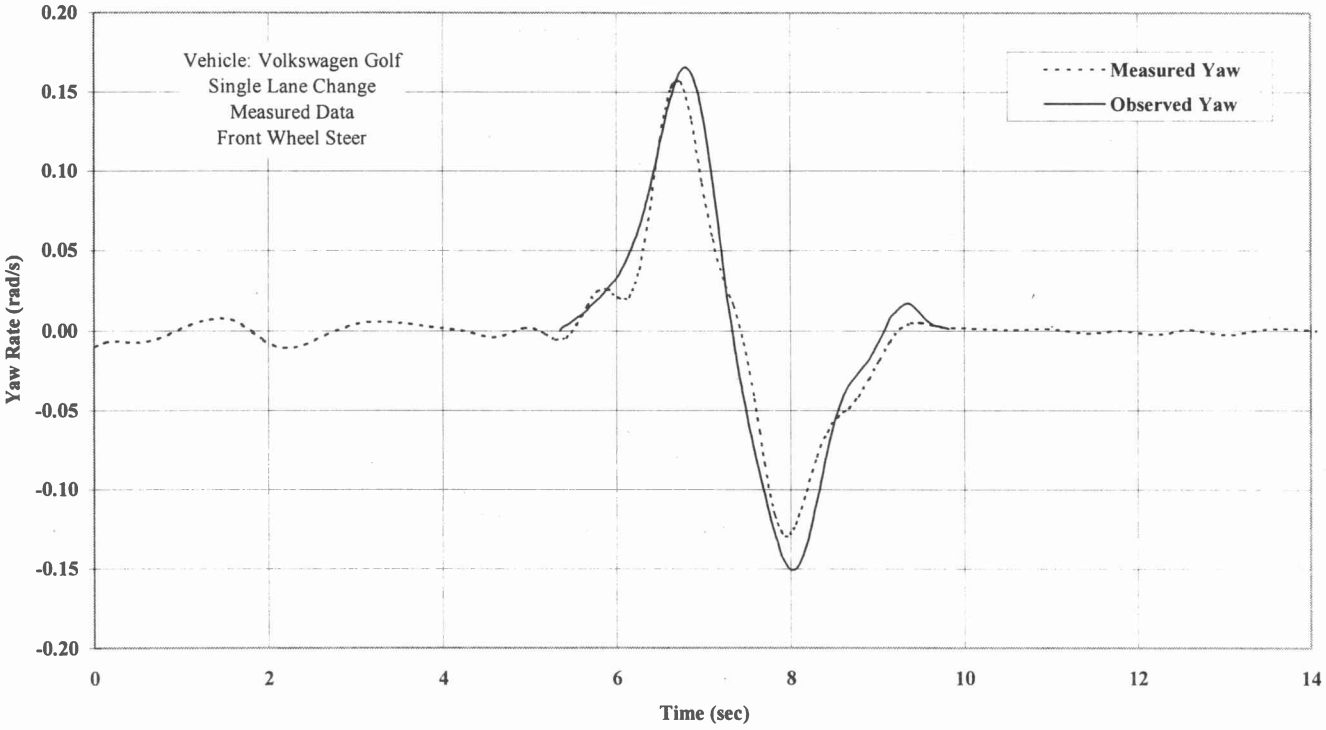

Figure 11 Performance of the observer in tracking the yaw rate of an actual vehicle from experimental data

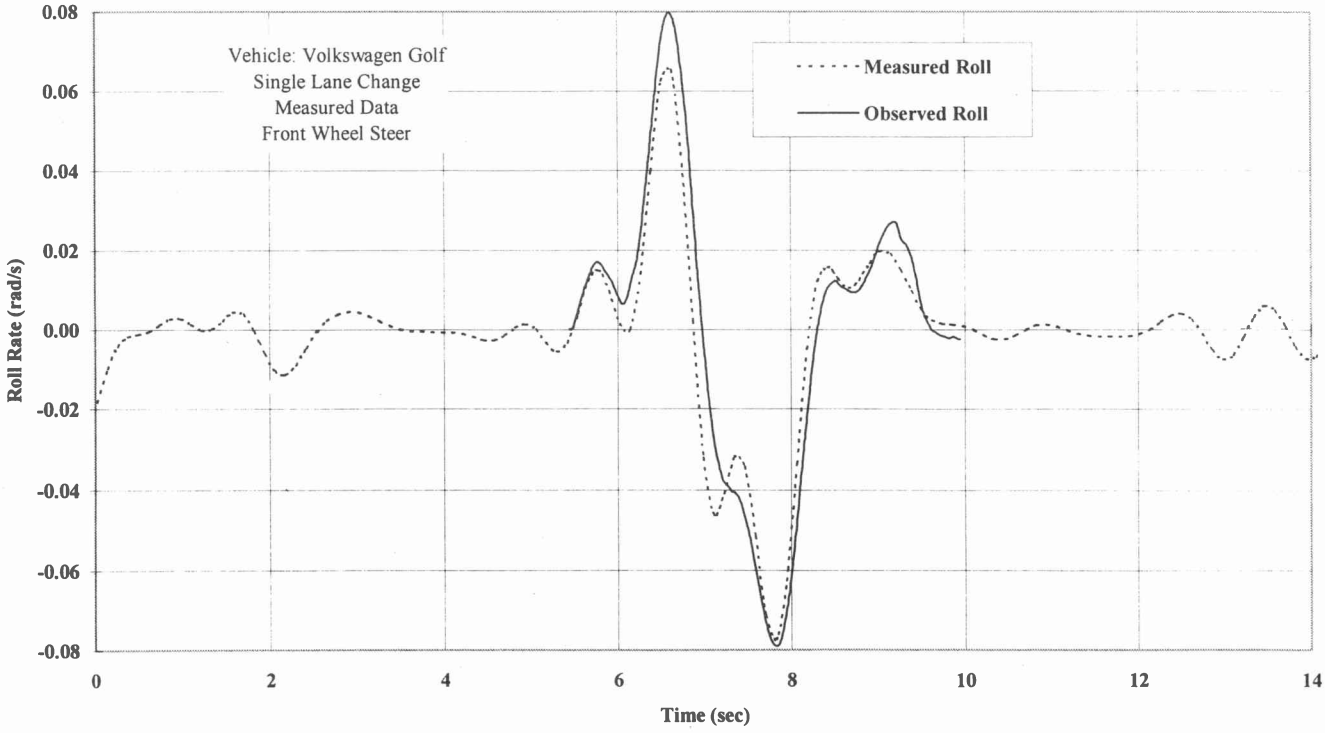

Figure 12 Performance of the observer in tracking the roll rate of an actual vehicle from experimental data

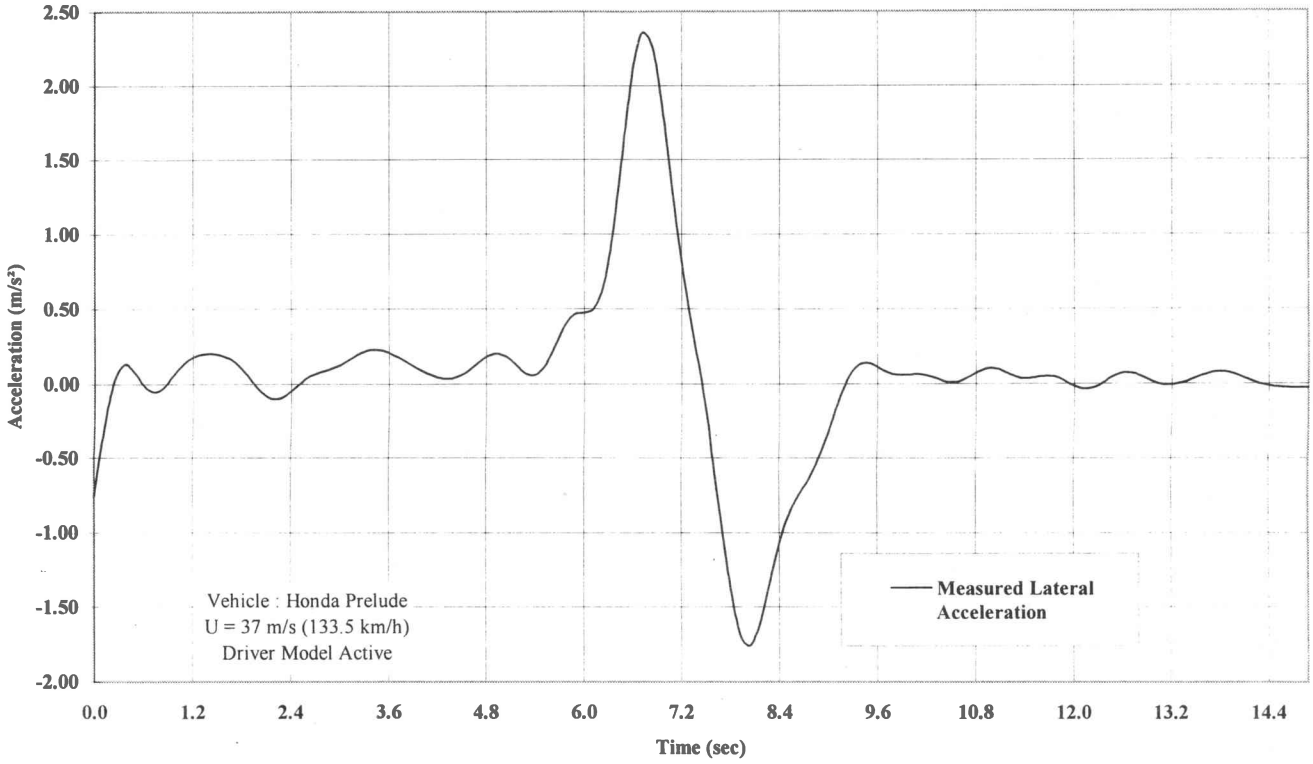

Figure 13 Measured lateral acceleration used as input to observer

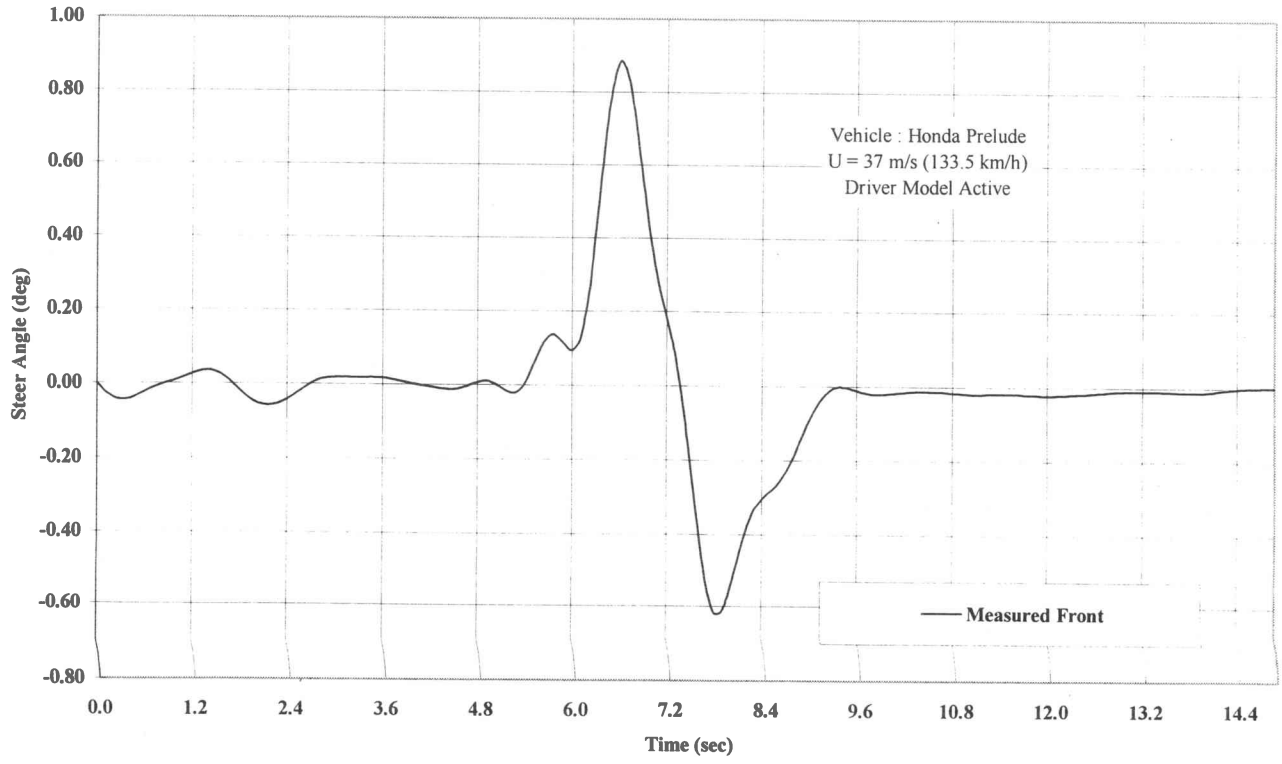

Figure 14 Measured steering angle used as input to observer

and the placement of the closed loop poles can have far-reaching implications. It is required to use the available knowledge of the inter-dependency between the different states when choosing the gains for the error feedback.

The linear observer does have limitations when observing non-linear vehicles. Most notable is the fact that the tyres are modelled as linear components which influence the observer's ability to estimate the vehicle states during severe manoeuvres. Furthermore, it is important to obtain accurate tyre characteristics when data from actual vehicle tests are used to ensure reasonable convergence between actual and observed vehicle states.

The real solution to this problem will be to implement an observer that is truly non-linear. However, as a first iteration this linear observer proves to be accurate even during very severe handling conditions and can produce reliable results.

References

1. Yu S *et al.* A Global Approach to Vehicle Control: Coordination of Four-Wheel Steering and Wheel Torques. *Journal of Dynamic Systems, Measurement, and Control*, **116**, 1994, pp.659–667.
2. Hirano Y *et al.* Development of Integrated System of 4WS and 4WD by H_∞ Control. *SAE Paper* 930267, 1993.
3. Hurdwell R *et al.* Active Suspension and Rear-Wheel Steering Make Powerful Research and Development Tools. *SAE Paper* 930266, 1993.
4. Aga M *et al.* Design of a Two-Degree of Freedom Control System for Active Front-And-Rear-Wheel-Steering. *SAE Paper* 901746, 1990.
5. Ohnuma A *et al.* Controllabilty and Stability Aspects of Actively Controlled 4WS Vehicles. *SAE Paper* 891977, 1989.
6. Constantine CJ *et al.* The Effects of Roll Control for Passenger Cars during Emergency Manoeuvres. *SAE Paper* 940225, 1994.
7. Shiotsuka T *et al.* Active Control of Drive Motion of Four-Wheel-Steering Car with Neural Network. *SAE Paper* 940229, 1994.
8. Senger JM *et al. Investigations on State Observers for the Lateral Dynamics of Four-Wheel-Steered Vehicles.* DLR Institute for Flight System Dynamics.
9. Kleine S. *Active Control of a Four-Wheel-Steered Vehicle.* Masters dissertation, University of Pretoria, 1996.
10. Von Riekert P *et al.* Zur Fahrmechanik des Gummibereiften Kraftfahrzeugs. *Ingenieur Archiv*, **11**, 1940, pp.659–667.
11. Allen RW, Rosenthal TJ & Szostak HT. Steady State and Transient Analysis of Ground Vehicle Handling. *SAE Paper* 870495, 1987.
12. Whitehead JC. Four-Wheel Steering: Manoeuvreability and High Speed Stabilization. *SAE Paper* 880642, 1988.
13. Nalecz AG *et al.* Handling Properties of Four Wheel Steering Vehicles. *SAE Paper* 890080, 1989.
14. Dugoff H *et al.* An analysis of tyre traction properties and their influence on vehicle dynamic performance. *SAE Paper* 700377, 1970.
15. Heydinger GJ *et al.* The Importance of Tire Lag on Simulated Transient Vehicle Response. *SAE Paper* 910235, 1991.
16. Friedland B. *Control System Design. An Introduction to State-Space Methods.* McGraw-Hill International Editions, New York, 1987.
17. Allen RW & Rosenthal TH. A Computer Simulation Analysis for Safety Critical Manoeuvres for Assessing Ground Vehicle Dynamic Stability. *SAE Paper* 930760,1993.

Appendix

The equations of motion for the three degree of freedom vehicle model are as follows:

$$\mathbf{M}\ddot{\mathbf{q}} + \mathbf{E}\dot{\mathbf{q}} + \mathbf{K}\mathbf{q} = \mathbf{F}\mathbf{u} \tag{29}$$

Where the matrices are defined as follows:

$$\mathbf{K} = \begin{bmatrix} 0 & 0 & 0 \\ 0 & K_\phi - M_s g z_t & 0 \\ 0 & 0 & 0 \end{bmatrix} \tag{30}$$

$$\mathbf{E} = \begin{bmatrix} \frac{C_0}{U} & 0 & MU + \frac{C_1}{U} \\ 0 & C_\phi & M_s z_t U \\ \frac{C_1}{U} & 0 & \frac{C_2}{U} \end{bmatrix} \tag{31}$$

$$\mathbf{F} = \begin{bmatrix} 2C_{\alpha f} & 2C_{\alpha r} \\ 0 & 0 \\ 2aC_{\alpha f} & -2bC_{\alpha r} \end{bmatrix} \tag{32}$$

$$\mathbf{M} = \begin{bmatrix} M & M_s z_t & 0 \\ M_s z_t & I_{xx} & I_{xz} \\ 0 & I_{xz} & I_{zz} \end{bmatrix} \tag{33}$$

where $\mathbf{q} = [y \quad \phi \quad \psi \quad v \quad p \quad r]^T$ and $\mathbf{u} = [\delta_f \quad \delta_r]^T$.

The conversion to state space format is done as follows

$$\mathbf{B} = \begin{bmatrix} \mathbf{0} \\ -\mathbf{M}^{-1}\mathbf{F} \end{bmatrix} \tag{34}$$

$$\mathbf{A} = \begin{bmatrix} \mathbf{0} & \mathbf{I} \\ \mathbf{M}^{-1}\mathbf{K} & \mathbf{M}^{-1}\mathbf{E} \end{bmatrix} \tag{35}$$

To determine the lateral acceleration from the vehicle states the **C** and **D** matrices are defined from the equation for lateral acceleration. If the component terms of the equation for lateral acceleration are written out in full the origin of these matrices can be seen, thus writing roll and yaw rate as:

$$\dot{v} = A_{41}y + A_{42}\phi + A_{43}\psi + A_{44}v + A_{45}p + A_{46}r + B_{41}\alpha_f + B_{42}\alpha_r \quad (36)$$

$$\dot{p} = A_{51}y + A_{52}\phi + A_{53}\psi + A_{54}v + A_{55}p + A_{56}r + B_{51}\alpha_f + B_{52}\alpha_r \quad (37)$$

these matrix coefficients terms originate from equation (34) and (35). Grouping terms and substituting into (13) results in:

$$a_y = \mathbf{C_a x} + \mathbf{D_a u} \quad (38)$$

where

$$\mathbf{C}_a = \begin{bmatrix} (A_{41} + z_t A_{51})(A_{42} + x_t A_{52})(A_{43} + z_t A_{53}) \\ (A_{44} + z_t A_{54})(A_{45} + z_t A_{55})(A_{46} + z_t A_{56} + U) \end{bmatrix} \quad (39)$$

$$\mathbf{D}_a = [(B_{41} + z_t B_{51})(B_{42} + z_t B_{52})] \quad (40)$$

which can be redefined as the **C** and **D** matrix in the state space model.